



University of HUDDERSFIELD

University of Huddersfield Repository

Colley, Gareth, Mishra, Rakesh, Rao, H.V. and Woolhead, R.

Performance evaluation of three cross flow vertical axis wind turbine configurations.

Original Citation

Colley, Gareth, Mishra, Rakesh, Rao, H.V. and Woolhead, R. (2009) Performance evaluation of three cross flow vertical axis wind turbine configurations. In: Proceedings of Computing and Engineering Annual Researchers' Conference 2009: CEARC'09. University of Huddersfield, Huddersfield, pp. 130-136. ISBN 9781862180857

This version is available at <http://eprints.hud.ac.uk/6881/>

The University Repository is a digital collection of the research output of the University, available on Open Access. Copyright and Moral Rights for the items on this site are retained by the individual author and/or other copyright owners. Users may access full items free of charge; copies of full text items generally can be reproduced, displayed or performed and given to third parties in any format or medium for personal research or study, educational or not-for-profit purposes without prior permission or charge, provided:

- The authors, title and full bibliographic details is credited in any copy;
- A hyperlink and/or URL is included for the original metadata page; and
- The content is not changed in any way.

For more information, including our policy and submission procedure, please contact the Repository Team at: E.mailbox@hud.ac.uk.

<http://eprints.hud.ac.uk/>

PERFORMANCE EVALUATION OF THREE CROSS FLOW VERTICAL AXIS WIND TURBINE CONFIGURATIONS

¹G.R. Colley, R. Mishra, H.V. Rao, R.Woolhead
University of Huddersfield, Queensgate, Huddersfield, HD1 3DH, United Kingdom

ABSTRACT

The performance output of three Vertical Axis Wind Turbine (VAWT) configurations has been evaluated using a two-dimensional Computational Fluid Dynamic (CFD) model. Data has been obtained using a quasi-steady Multi Reference Frame (MRF) approach in which the three variants were subjected to an inlet velocity of 4m/s and rotor blade tip speed ratios (λ) in the range of 0 to 0.6. The results obtained show a clear reduction in torque output as both the number of stator and rotor blades decrease. Furthermore, the power output of for each configuration reduces as a function of a reduction in number of stator/rotor blades.

Keywords: Vertical axis wind turbine, CFD, Performance.

INTRODUCTION

The need for sustainable energy sources becomes greater each year due to the continued depletion of fossil fuels. To harness such types of energy wind turbines are now seen as the most logical choice due to their well established performance credentials along with relatively short payback times. Among the different types of wind turbines, the most common type is Horizontal Axis (HAWT) in which the primary axis of rotation is parallel to the ground. Another type of wind turbine in use is the vertical axis in which its rotational axis is normal to the ground. The main attraction of the Vertical Axis Wind Turbines (VAWT) is the simplicity of the design which allows for energy conversion at any wind angle. Furthermore its requirement of low starting torque coupled with low noise make it an ideal candidate for use within urban areas where wind speeds are relatively low [1,2,3].

Vast amounts of research have been carried out on VAWTs particularly Savonius and Darrieus types with the aim of identifying the optimum geometric configuration for maximum power output [4,5,6,7]. In this research three types of cross flow multi blade VAWT have been evaluated to maximize the performance output. The nature of flow through cross flow impellers/turbines such as 'Banki' is well documented and has been shown to be asymmetric despite its geometrical symmetry about the axis of rotation. Due to this phenomenon, performance prediction of these turbines using standard models has proven to be difficult. In this work a two-dimensional Computational Fluid Dynamic (CFD) study has been undertaken using a Multi Reference Frame (MRF) solving technique to evaluate the performance of these configurations under various rotational conditions.

The performance of many small scale VAWTs has been evaluated over the past decade however the Savonius and Darrieus type turbines are still the most widely recognized amongst all VAWTs. The use of external flow conditioning devices such as stator arrays has recently been documented [14]. The performance benefits of such devices are still widely unknown with little literature available. The current research has been undertaken to provide a comparative study of different VAWT blade configurations with the aim of understanding the performance effects of each. The works cited in this research provide a well documented evaluation of current VAWTs that are either at a prototype or production stage. It is clear that further work is needed to fully understand the effects of such devices along with the complexities of the through flow inherent with this design [8,9,10,11,12,13,15].

2 PERFORMANCE PARAMETERS

Blade Tip Speed Ratio (TSR)

The blade tip speed ratio (λ) has been used in the present analysis to obtain optimum operating condition for the wind turbine. It is defined as the ratio of circumferential velocity of the turbine to the wind velocity. The following equation has been used to calculate the tip speed ratio.

$$\text{Eq.1} \quad \lambda = \frac{\omega \cdot r}{V}$$

ω \equiv Angular rotational velocity of the rotor (rad/s)
 r \equiv outer radius of the turbine rotor (m)
 V \equiv flow velocity (m/s)

The other parameters used in the analysis have been defined in the text and the nomenclature section.

3 COMPUTATIONAL PARAMETERS

The CFD software Fluent numerically simulates a virtual flow domain for a given application. It iteratively solves the time-averaged Navier-Stokes equations along with the continuity and auxiliary equations using a control volume approach. The finite volume approach has been used to divide the computational domain into a number of control volumes (cells). The governing differential equations are then expressed in the form of general transport equation consisting of convection, diffusion and source terms. The transport equations are integrated over all the finite control volumes. Finite-difference-type substitutions are made for the various terms in these integrated equations, resulting in a set of algebraic equations for the flow parameters. The flow parameters are then numerically solved using suitable iterative methods for the simultaneous algebraic equations. Figure.1 shows the computational grid used for these simulations.

Due to the rotational motion of the rotor, the flow field in and around the rotor is complex. However, since the flow field within the rotor is of interest for this investigation (torque output), the cell zones corresponding to the rotor were defined using MRF approach. This allowed the flow field around the moving rotor to be considered as quasi-steady. This is accomplished in the CFD code by incorporating additional acceleration terms which occur due to the transformation from the stationary to the moving reference frame. The flow around the rotor could then be modelled by solving the transport equations in a steady-state manner. The boundary conditions for the rotor fluid are generated by averaging the interface condition between the rotor and the stator.

In the present work the RNG k- ϵ turbulence model [16] was chosen to resolve the steady-state turbulent parameters in the flow domain. The boundary conditions of the flow domain have been defined to represent practical turbine operating conditions and are shown in Figure.1. The inlet of the computational flow domain was defined as a 'velocity inlet' boundary condition, in which a constant normal velocity of 4m/s was used in the positive X axis direction. To ensure accurate data has been obtained a second order discretization scheme has been used for the convection terms of each governing equation. This is due to the tetrahedral grid used as the flow is never aligned with the grid. If a first order scheme was used, large numerical diffusion would occur which would result in large inaccuracies. Furthermore a node based gradient averaging scheme has been used due to its higher accuracy when compared to cell based for unstructured grids. Finally a convergence criterion of 10^{-5} has been used for each of the turbine configurations.

4 RESULTS & DISCUSSION

The following results have been obtained using an identical grid for each configuration using an inlet velocity of 4m/s which is common to all. Furthermore the rotor blade tip speed ratio (λ) (defined in Eq.1) has been varied from 0 – 0.6 in increments of 0.1 at a constant radius of 0.7m.

12 STATOR/12 ROTOR

In this configuration an array of 12 equally spaced stator blades have been used to condition the flow for optimum inlet angles before it enters the rotor assembly. In this instance an equal number of equally spaced rotor blades have also been used as depicted by Figure.2.

The complex pressure and flow velocity distributions at $\lambda=0.1$ within the turbine have been computed in Figures.3 and 4. Here the asymmetry as reported by 'Yamafuji' [11] can be clearly seen. Furthermore, areas of recirculating flow can also be observed. It has been reported by Klemm et al [9] that these regions of recirculation result in a reduction in energy transfer due to the small vortices present. The contour plot (Figure.3) depicts the static pressure variation around the turbine structure in the XY plane. From this figure certain interesting flow field characteristics can be identified. The regions which are circled black, show areas of low pressure which are present within the blade passageways. These low pressure regions generally cause disruption to the flow and ultimately results in the creation of secondary flows such as re-circulation which are detrimental to the energy transfer process.

The contours of velocity magnitude (Figure.4) clearly show which regions within the wind turbine experience high levels of flow. A trend visible from this figure is that low velocity is often present behind a blade. This is due to the blade orientation relative to the flow in the X direction. It can be seen that the blades with orientations close to being normal to the flow generate a low velocity region downstream. This is due to the blade restricting the air flow from entering into the adjacent blade passageway thus resulting in a low velocity magnitude region.

The resultant pressure field due to a blades orientation relative to the flow has a direct effect on the turbines performance output. The pressure differential across a rotor blade results in a rotational moment about the central axis of rotation. Furthermore, it is fair to say that blade passages allowing a higher mass flow rate of air are likely to generate the most amounts of torque. The following figure shows the torque variation as a function of angular velocity. Here, λ has been varied from 0-0.6 in increments of 0.1, which equates to rotor angular velocities of 0, 0.57, 1.14, 1.71, 2.29, 2.86, 3.43 rad/s respectively.

It can be seen from Figure.5 that the torque output of the wind turbine decreases as rotational speed increases. The turbine generates a maximum torque of 18.2Nm when the rotor assembly is static. The peak torque present under rotational conditions is 15.13Nm at $\lambda=0.1$. It can be seen from the turbine power curve that the power output of the turbine increases as a function of λ up to 0.4. At this tip speed ratio the turbine generates a power of approximately 19.29W. Beyond this tip speed ratio the power output begins to decrease at a steady rate. Based on this data the turbine should be kept at an operating speed of between 1.71 - 2.86 rad/s for optimum power generation. This assumption however is based on an unloaded condition in which transmission effects have not been quantified.

6 STATOR/6 ROTOR

The following section describes the results obtained for the second turbine configuration. Figure.7 shows the blade configuration in which 6 equally spaced stators and rotors have been used. To understand the effect of this geometry on the local flow field, contours of pressure and velocity magnitude have been obtained. From Figure.8 it is evident that the local pressure distribution around the wind turbine has changed considerably when compared to that of configuration 12/12. The flow field within the turbine is now less complex due to reduced geometrical influences on the flow. Further, the pressure field still has similar trends in that high and low pressure regions exist at similar positions as highlighted in the figure. Similar trends can also be observed in Figure.9 in which low velocity regions are again present downstream of turbine blades causing most disruption to the flow. In this instance due to the reduced number of blades there is a much greater through flow through the core (centre) of the turbine as highlighted on the contour plot.

It is evident that the torque variation of this type of turbine (Figure.10) when compared to the 12/12 configuration behaves in a similar manner. Again the torque output of the turbine decreases as a function of λ up to 0.6 where it actually becomes negative. The maximum torque generated in this instance is 8.3 Nm for a static condition which is 54.4% less than the 12/12 configuration. The maximum torque generated under rotational conditions is in the order of 6.54Nm @ $\lambda=0.1$ which is a 56.8% decrease on the previous configuration. These reductions of approximately 50% clearly have a relation with the fact that this configuration has 50% less blade area.

The power curve for this turbine is depicted by Figure.11; the characteristics of the curve have some similarities when compared to the first turbine configuration. Here the power output rises as the tip speed ratio of the rotor increases from 0 to 0.3 where it reaches a peak power of 6.43W. With this in mind the point at which the turbine generates peak power has now shifted when compared to the first configuration. The maximum power generated is also 62.81% down in comparison.

3 STATOR/3 ROTOR

The final configuration that has been tested contains three stator blades and three rotor blades (Figure.12) equally spaced about the turbines central axis of rotation. Contours of static pressure and velocity magnitude have again been computed at a velocity of 4m/s and λ of 0-0.6.

The contours of static pressure depicted by Figure.13 show a much simpler distribution due to the reduction in turbine blades (flow obstructions). In this instance high pressure regions still exist at the stator blade surfaces along with low pressure downstream of the blades. The contours of velocity magnitude (Figure.14) again show similar trends when compared to the previous two configurations. It can be seen that a large flow of air is present through the core of the turbine and is relatively un-disturbed. The highlighted regions again show low velocity zones due to the orientation of the blades relative to the flow direction.

The performance of this turbine has been quantified in relation to the initial 12 stator/12 rotor configuration in which torque and power output have both been computed. Figure.15 depicts the variation of torque output in relation to λ . It can be seen that the torque again decreases as a function of an increase in λ where it becomes negative beyond $\lambda=0.4$. The maximum torque is generated when the rotor is static (4.215Nm) and 3.32Nm at $\lambda=0.1$. This sees a reduction of 76.84% and 78.05% when compared to the first configuration.

The power curve shown in Figure.16 has different characteristics when compared to those of the previous configurations. The point at which peak power is produced has again shifted to a lower rotational speed at $\lambda=0.2$. The peak power generated for this configuration is in the order of 2.5W and operates at its optimum between $\lambda=0.1$ and $\lambda=0.3$. This peak power is 85.53% less than the peak power observed in the first configuration.

5 CONCLUSIONS

- It can be seen that the torque output of each turbine decreases as a function of an increase in rotor tip speed ratio (λ).
- Peak power output of each configuration decreases as a function of a reduction in stator/rotor blade number.
- The point at which peak power is generated is dependent on the number of blades used.

•

NOMENCLATURE

p = Pressure (Pa)
 ρ = Air Density (kg/m^3)
 Q = Mass flow rate (kg/s)
 V = Velocity (m/s)
 ω = Angular Velocity (rad/s)
 λ = Tip Speed Ratio
 P = Power (W)
 T = Torque (Nm)
 r = Turbine radius (m)
 h = Turbine height (m)

REFERENCES

- [1] J.Walker (2009), Renewable energies: How far can they take us?
 [2] BTM Consultants (2008), World market update 2007.
 [3] J.K.Lemming et al (2009), Future wind energy technology and CO2 perspectives.
 [4] Global Wind Energy Council (GWEC) (2007), Global wind report 2007.
 [5] S.Erikson, H.Bernhoff and M.Leijon (2006), Evaluation of different turbine concepts for wind power.
 [6] H.Riegler (2003), Re-focus, HAWT Vs VAWT.
 [7] T.Sankar, The case for vertical axis wind turbines.
 [8] P.R.Tuckey et al (1982), Performance and aerodynamics of a cross flow fan.
 [9] T.Klemm et al (2007), Application of a cross flow fan as a wind turbine.
 [10] A.Toffollo (2004), An experimental investigation of the flow field pattern within the impeller of a cross flow fan.
 [11] K.Yamafuji (1975), Studies on the flow of cross flow impellers.
 [12] J.A.V.Ale et al (2007), Performance evaluation of the next generation of small vertical axis wind turbine.
 [13] S.Tullis et al (2007), Medium-solidity Vertical Axis Wind Turbines for use in urban areas.
 [14] F.Kamal and Q.Islam (2008), Aerodynamic characteristics of a stationary five bladed vertical axis vane wind turbine..
 [15] J.Y.Park et al (2007), A novel vertical axis wind turbine for distributed & utility deployment.
 [16] Fluent User Guide (2006)

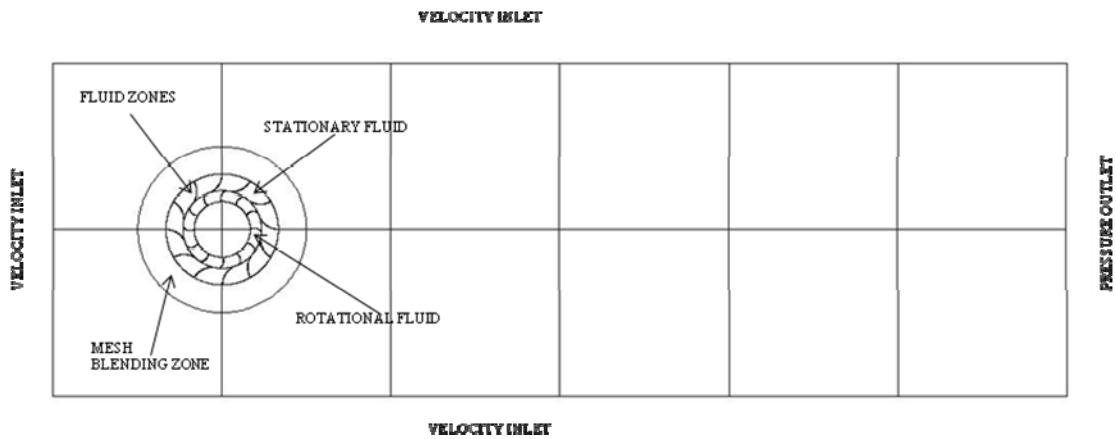


Figure.1 'Computational grid for 12 stator/12 rotor configuration'

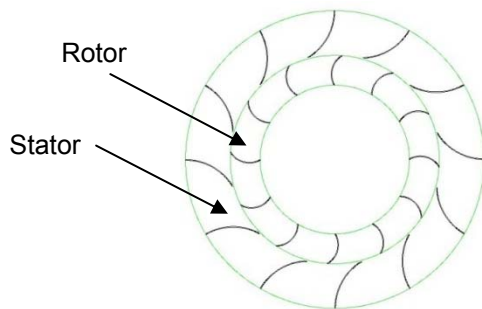


Figure.2 '12 stator/12 rotor configuration'

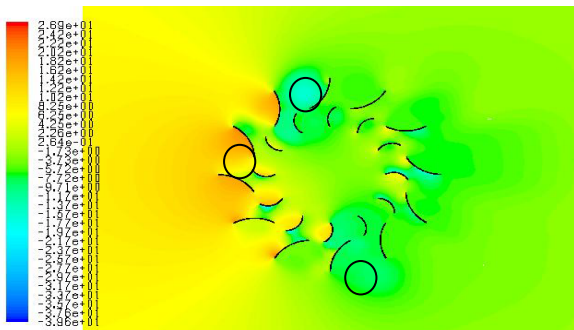


Figure.3 'Contours of static pressure for an operating condition of 4m/s and rotational speed of 0.57rad/s'

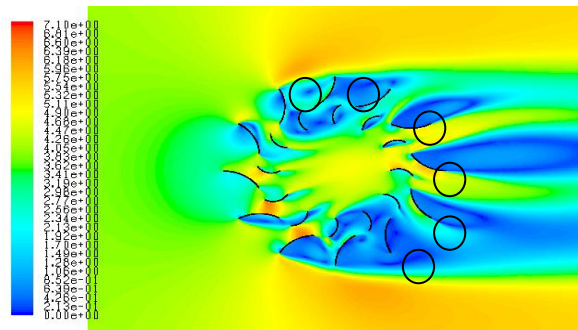


Figure.4 'Contours of velocity magnitude for an operating condition of 4m/s and rotational speed of 0.57rad/s'

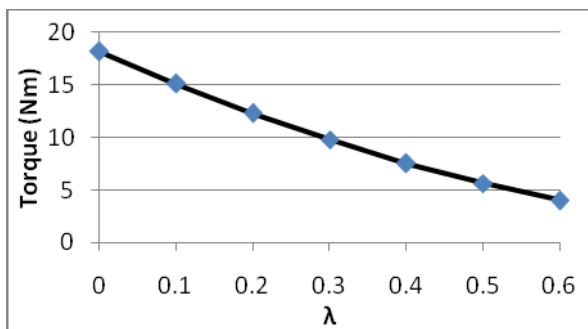


Figure.5 'Variation of turbine torque output as a function of λ '

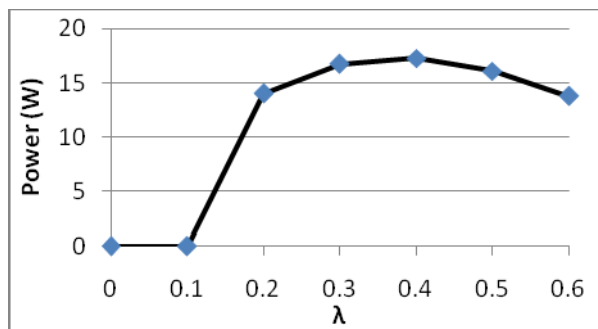


Figure.6 'Variation of turbine power output as a function of λ '

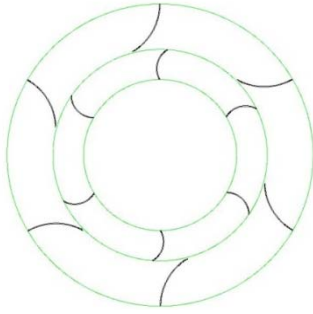


Figure.7 '6 stator/6 rotor configuration'

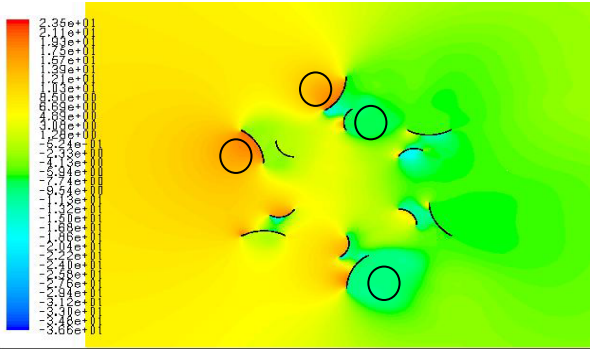


Figure.8 'Contours of static pressure for an operating condition of 4m/s and rotational speed of 0.57rad/s'

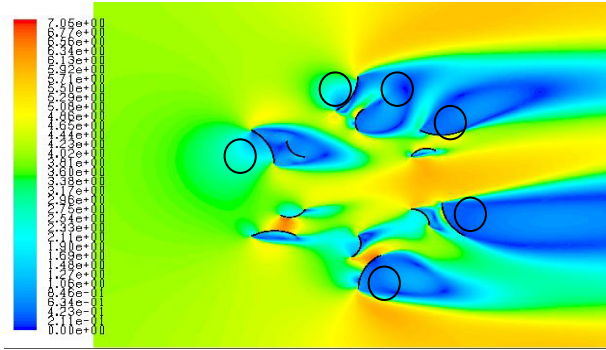


Figure.9 'Contours of velocity magnitude for an operating condition of 4m/s and rotational speed of 0.57rad/s'

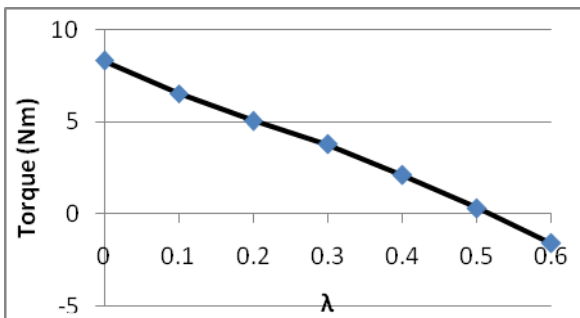


Figure.10 'Variation of turbine torque output as a function of λ '

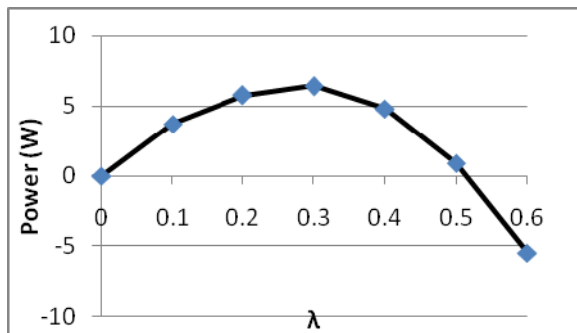


Figure.11 'Variation of turbine power output as a function of λ '

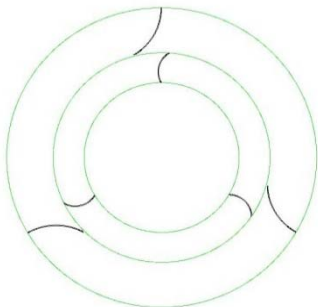


Figure.12 '3 stator/3 rotor configuration'

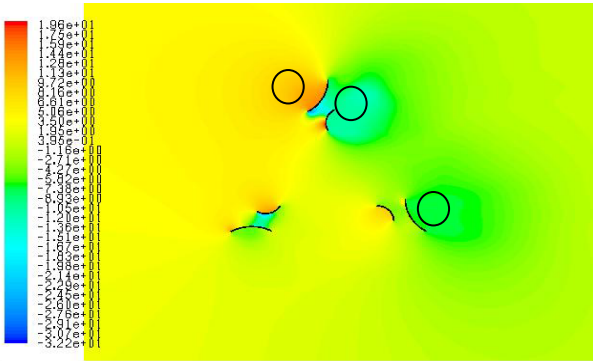


Figure.13 'Contours of static pressure for an operating condition of 4m/s and rotational speed of 0.57rad/s'

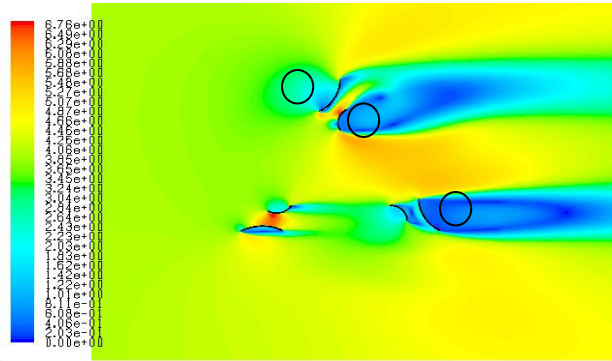


Figure.14 'Contours of velocity magnitude for an operating condition of 4m/s and rotational speed of 0.57rad/s'

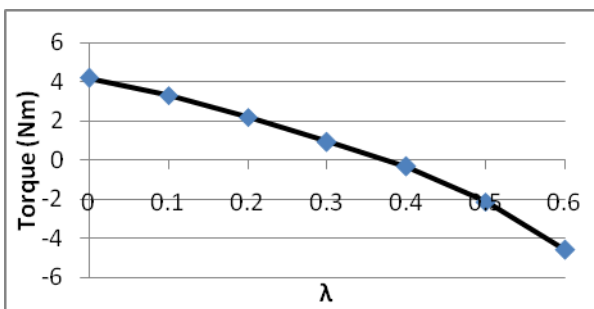


Figure.15 'Variation of turbine torque output as a function of λ '

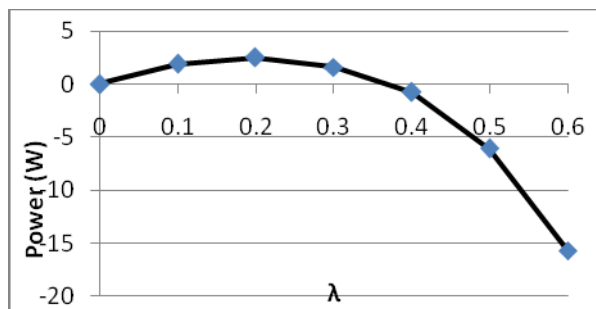


Figure.16 'Variation of turbine power output as a function of λ '